Journal of Alloys and Compounds 446–447 (2007) 52–57

Journal of ALLOYS AND COMPOUNDS

www.elsevier.com/locate/jallcom

Nanostructured magnesium hydride for pilot tank development

P. de Rango [a,b,*], A. Chaise [a,b], J. Charbonnier [a,b], D. Fruchart [a], M. Jehan [c],
Ph. Marty [d], S. Miraglia [a], S. Rivoirard [b], N. Skryabina [e]

[a] *Laboratoire de Cristallographie, CNRS, BP166, 38042 Grenoble Cedex 9, France*
[b] *Consortium de Recherché pour l'Emergence de Technologies Avancées, CNRS, BP166, 38042 Grenoble Cedex 9, France*
[c] *MCP Technologies SA, rue Vaucanson, 26100 Romans sur Isère, France*
[d] *Laboratoire des Ecoulements Géophysiques et Industriels, CNRS, BP53, 38041 Grenoble, France*
[e] *Department of Physics, Perm State University, 15 Bukireva, Perm 614990, Russia*

Received 12 September 2006; received in revised form 17 January 2007; accepted 18 January 2007

Abstract

The aim of the present work was a systematic investigation on MgH_2 co-milled with transition metals M, in order to develop large batches of suitable materials for hydrogen storage. Systematic ball-milling operations were done using a planetary miller, thus leading to combine the transition metal with MgH_2 to form successive MH_x hydrides. The initiating role of the metal hydride MH_x was evidenced by in situ neutron diffraction experiments. The co-milling conditions were transferred to MCP Technologies SA, where highly reactive batches of powders were processed. These powders appear to be very stable on cycling, provided the desorbed powders are not exposed to a temperature higher than 370 °C. A small scale MgH_2 tank was developed. Absorption and desorption cycles have been operated in different experimental conditions.

Keywords: Hydrogen absorbing materials; Metal hydrides; Mechanical alloying; Computer simulations

1. Introduction

Magnesium hydride MgH_2 is an excellent material for hydrogen storage: it is abundant, cheap, and presents a high storage capacity by weight (7.6 wt.%). Its limitation for practical applications, however, lies in both slow hydrogen sorption kinetics and high thermodynamic stability ranges. Many attempts have been done to improve these properties. It has been shown that nanocrystalline MgH_2 formed by intense ball milling leads to more improved properties than conventional polycrystalline MgH_2 [1]. A second improvement has been obtained by the introduction of transition elements such as Ti, V, Mn, etc. which act as catalysts to further enhance the sorption kinetics of MgH_2 [2,3]. Oelerich et al. have shown that transition metal oxides additions are very efficient too [4]. Up to now, despite its high storage capacity, very few attempts of tank conception have been carried out with magnesium-based alloys. Most of the reactors studied contain conventional $LaNi_5$ based alloys to validate associated numerical models [5–8]. The aim of the present work is a systematic investigation of the co-milling process with transition metals, in order to develop both large batches of suitable materials for hydrogen storage and a small scale MgH_2 tank, in order to demonstrate that MgH_2 can be use for practical applications.

2. Experimental

Pure MgH_2 (95% MgH_2, 5% Mg) was provided by MCP Technologies SA. Transition elements M (M = Ti, V, Nb) were introduced into the form of fine powders (typically 40 μm). Intensive ball-milling operations were done at the laboratory scale using a planetary Fritsch miller. The 250 cm^3 tempered steal pots were sealed in glove box, and the ball to powder ratio was of 50:1. All handling was also performed in a glove box under argon atmosphere. X-ray diffraction analysis was carried out using a Siemens D5000 X-ray diffractometer with Cu Kα radiation. In situ neutron diffraction experiments under deuterium pressure were performed at ILL-Grenoble (D20), using a dedicated furnace. A multicounter detector allows diffraction diagrams to be recorded every 5 min during the hydrogenation. Particles size measurements were performed using a laser granulometer (Malvern Mastersizer 2000). A Philips 300 kV HREM was used for nanostructural observations. The hydrogen absorption/desorption properties were measured with a HERA Sieverts device. To minimize the self-heating during hydrogen absorption, we test only 100 mg of powder with a stainless-steal sample-holders of 26 g.

---

[*] Corresponding author at: Laboratoire de Cristallographie, CNRS, BP166, 38042 Grenoble Cedex 9, France. Tel.: +33 4 76 88 90 30;
fax: +33 4 76 88 12 11.
E-mail address: patricia.derango@grenoble.cnrs.fr (P. de Rango).

0925-8388/$ – see front matter © 2007 Elsevier B.V. All rights reserved.
doi:10.1016/j.jallcom.2007.01.108

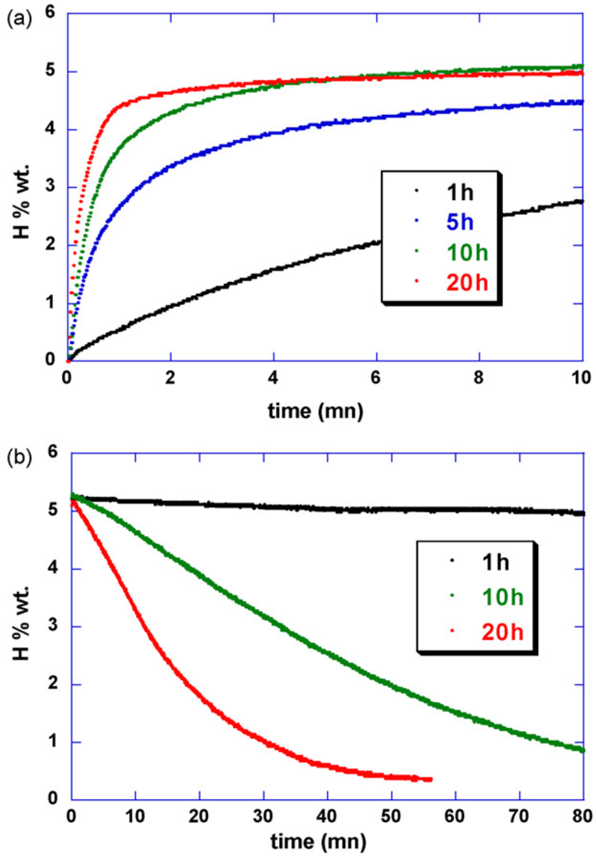

Fig. 1. MgH_2 powders ball milled for increasing durations in the planetary Fritsch miller, with 5 at.% vanadium powders. Kinetic traces of hydrogen (a) absorption under 1 MPa hydrogen pressure at 240 °C and (b) desorption under 15 kPa gas pressure at 240 °C.

3. Analysis of the milling process at laboratory scale

The milling process has been analysed for pure MgH_2 and for the addition of transition elements such as Ti, V and Nb. Absorption and desorption kinetics have been markedly improved, when using fine transition element powders (40 μm) instead of raw chips. MgH_2 powders with 5 at.% of vanadium powders have been ball-milled for increasing milling times ranging from 15 min to 60 h. A small amount of powder was sampled successively from the same milled batch for each measurement. As observed on Fig. 1a, the absorption kinetics increase rapidly between 1 and 5 h of milling, then remain rather similar for 10 and 20 h. On the contrary, the desorption kinetics, especially at low temperatures (240 °C and below) are very sensitive to the milling time. In these experimental conditions, 20 h of milling are needed to achieve good desorption kinetics (Fig. 1b).

3.1. Structural and microstructural evolutions during milling

Systematic and high-resolution XRD patterns were recorded on the processed powders. Similar behaviours were observed for all the transition elements M. After about 1 h of milling time, the metal M progressively transforms into MH_x ($0.65 < x < 0.9$) thus forming off-stoichiometric hydrides thanks to the MgH_2 mass.

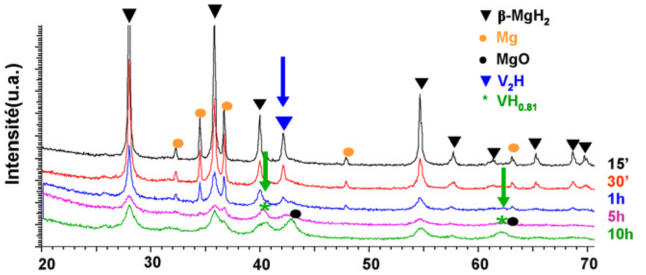

Fig. 2. X-ray diffraction patterns recorded for increasing milling times (MgH_2 + 5 at.% Nb).

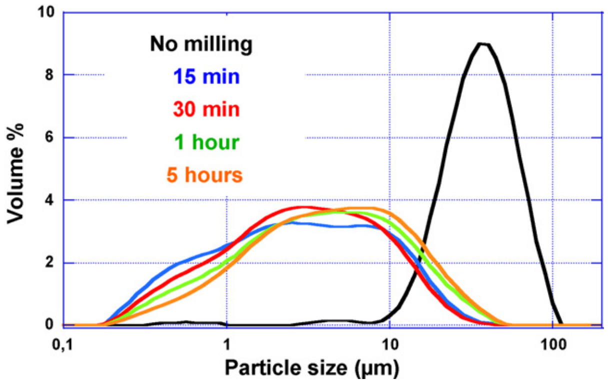

Fig. 3. Particle sizes recorded on (MgH_2 + 5 at.% Nb) powder milled for increasing milling times, ranging from 15 min to 5 h.

For example with Nb additions (Fig. 2), ε-$NbH_{0.7}$ is formed first after 30 min of milling time. Then after at least 10 h of milling, more and more loaded metal hydrides are formed (MH to MH_2) progressively, detrimental to the type of metal hydride formed first. Beside, a progressive increase of the XRD line width of the MgH_2 major phase is observed due to the formation of high densities of defects and reduction of the size of the crystallites. In parallel, weak lines of pure Mg and some traces of $Mg(OH)_2$ are observed for long MT (50–60 h). As a result of the reaction kinetics, 20 h of milling time are sufficient to get optimised reaction conditions. This specific milling length corresponds approximately to that required to fully hydride the metal additive, and could correspond to the achievement of a fully mechanical binding between MgH_2 and additive particles.

Particles size was systematically measured on the above processed powders (Fig. 3). Starting from a 20 to 80 μm particles size, in 15 min the milling procedure leads to particles which size is comprised between 1 and 10 μm. After 15 min of milling, the particles size was not reduced anymore. The size of individual β-MgH_2 crystallites was calculated using the Scherrer formula from the X-ray diffraction lines (Table 1). After 15 min of milling

Table 1
Crystallite sizes of the β-MgH_2 phase calculated using the Scherrer formula

Milling time	Crystallite sizes (nm)
15 min	29 (3)
30 min	14 (2)
1 h	12 (2)
5 h	10 (9)

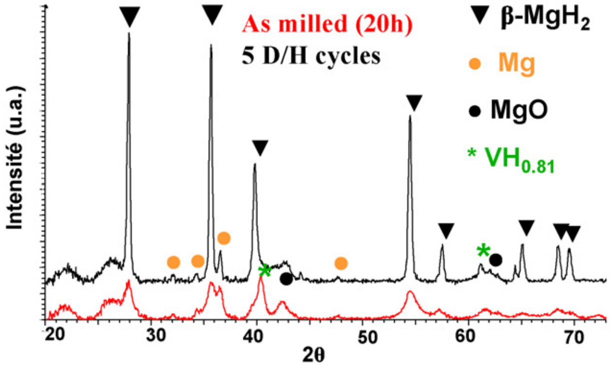

Fig. 4. X-ray diffraction patterns recorded after 20 h of milling (in red) and after five dehydrogenation/hydrogenation cycles (in black).

time, the crystallite size reaches about 30 nm but it continues to decrease for longer milling time.

3.2. *Structural and microstructural evolutions during hydrogen cycling*

The efficient milling process both reduces the size of the particles and produce large amounts of defects in the crystal structure (dislocations, grains defects, etc.). It results in a dramatic improvement of the reaction kinetics. It is four times faster for pure MgH_2 milled during 20 h than for un-milled MgH_2 samples to absorb 80% of the maximum hydrogen uptake. This means that for a significant part, the activation process could result from the induced defects and reduction of the particle size. However, the diffraction pattern recorded after five dehydrogenation/hydrogenation (D/H) cycles at 240 °C shows very narrow diffraction lines, as compared to the pattern recorded immediately after milling (Fig. 4). The partially amorphous state disappears after the first H/D cycles and the high density of defects induced during a long milling time is not directly responsible for the kinetics enhancement, since reproducible kinetics curves are observed for the further H/D cycles.

In order to better understand the basis of this process in terms of microstructural transformations, fully hydrogenated particles of magnesium were introduced in the chamber of a HREM after 20 h of milling time. The grain size of the MgH_2 particles was up to a tenth μm. Under the effect of both the high vacuum conditions in the microscope and the impact of the electron beam the hydride rapidly decomposes into pure Mg metal. Microscopy photographs and diffraction patterns were taken successfully, and reveal a net transformation between a homogeneous MgH_2 system into a mixture of MgH_2 and Mg nano-grains, and finally into desorbed grain composed of very well shaped hexagonal single crystallites of Mg. The size of the crystallites was established to cover a wide range from less than 5–40 nm as seen on Fig. 5. The corresponding diffraction pattern reveals a unique Mg system. It emphases that the rapid hydrogen diffusion in such milled and activated powders can be the result of the existence of numerous grains boundaries developed between nanometric crystallites. Then the ball milling induces a high density of defects as an intermediate state, which favors the recrystallisation of a fine nanostructured state.

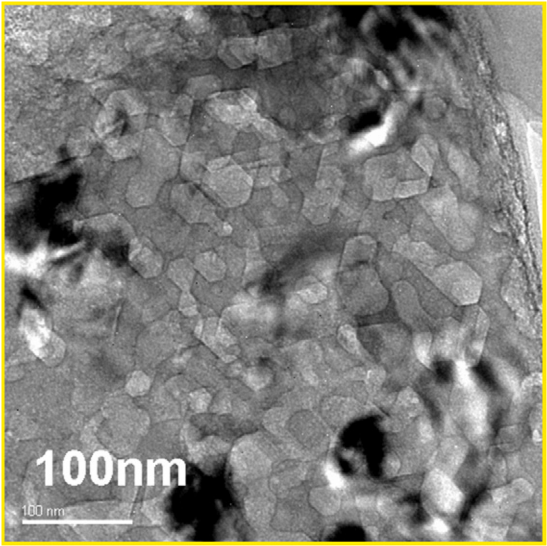

Fig. 5. A microscopy photograph obtained under HREM conditions after hydrogen desorption.

3.3. *Catalytic role of the transition elements*

In order to better understand the catalytic role of the additives on the hydrogen sorption, in situ neutron diffraction experiments were performed on nano-structured powders containing 5 at.% Nb. The powders were out-gassed prior to the neutron diffraction experiment. The successive patterns were recorded every 5 min during hydrogenation at 280 °C under 2 MPa of deuterium pressure. Fig. 6 clearly shows that the ε-$NbD_{0.7}$ phase (metastable under the applied conditions) has been formed first, prior to growth of MgH_2 particles. Thus the initiating role of the metal hydride MH_x was directly evidenced, in agreement with previous study based on synchrotron radiation experiments [9].

4. Up-scaling of the nanostructured MgH_2 production

The procedure to synthesise MgH_2 precursors in large amounts is now stated at MCP Technologies SA by solid gas reaction, using a commercial type autoclave installed in a rotary furnace. A protocol enabling the production of excellent MgH_2 powders, which appears almost saturated (no free Mg metal).

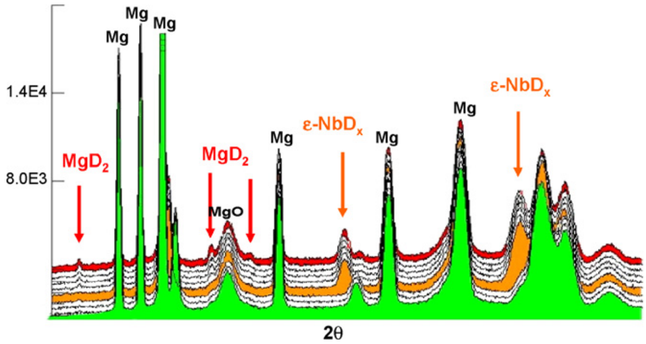

Fig. 6. Successive neutron diffraction patterns recorded in situ during hydrogenation (deuteration) process at 280 °C, 2 MPa D_2 gas pressure (MgH_2 + 5 at.% Nb milled for 20 h).

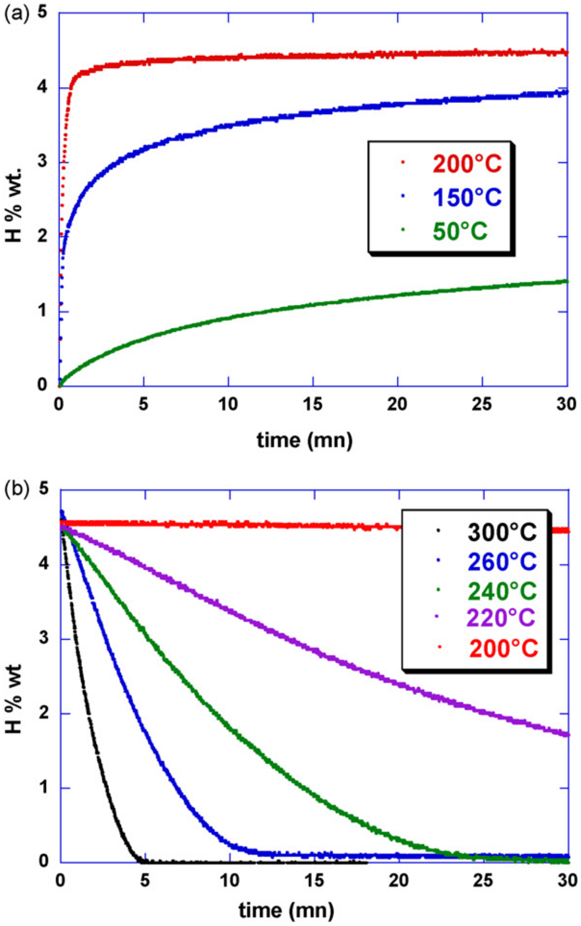

Fig. 7. Kinetic traces of (MgH_2 + 5 at.% V) powder ball milled for 8 h at MCP T. Hydrogen (a) absorption under 1 MPa H_2 pressure vs. temperature and (b) desorption under 15 kPa H_2 pressure.

The activating process at industrial scale is performed in a specific ball miller having a range of mechanical energy well adapted for rapid deliveries of M-activated MgH_2 powders. Such a 25 l machine enabled MCP Technologies SA to start the milling process of large batches of MgH_2 powder. Thanks to the optimisation of the milling conditions, very reactive powders have been prepared. As observed on Fig. 7a, and unexpectedly, hydrogen absorption can be effective at temperatures as low as 50 °C. Although kinetics remains rather low at this temperature, the exothermic absorption reaction induces an effective thermal activation. The increase of temperature, measured directly into the powder itself is about 25 °C at 150 °C. The desorption kinetics are slower than absorption ones. Nevertheless, at 220 °C and under 15 kPa (Fig. 7b), a complete desorption can be achieved within 1 h only.

Cycling at 300 °C the powders produced at MCP Technologies SA demonstrate a very high stability in the H/D characteristics. Moreover, it is possible to restore the powders when damaged by air exposure. An outgas specimen has been exposed to air atmosphere at 300 °C for 10 min. As observed on Fig. 8, the absorption curve recorded immediately after oxidation is strongly affected, whereas further cycles allowed reaching progressively the initial one. This phenomenon has been attributed to the formation of an oxide passivation layer at the surface of the grains, as already observed by Friedrichs et al. for all nanocrystalline magnesium samples [10]. This MgO layer first slows down the hydrogenation kinetics (especially during the 20 min of the first absorption) then split up under the effect of the expansion induce by hydrogenation.

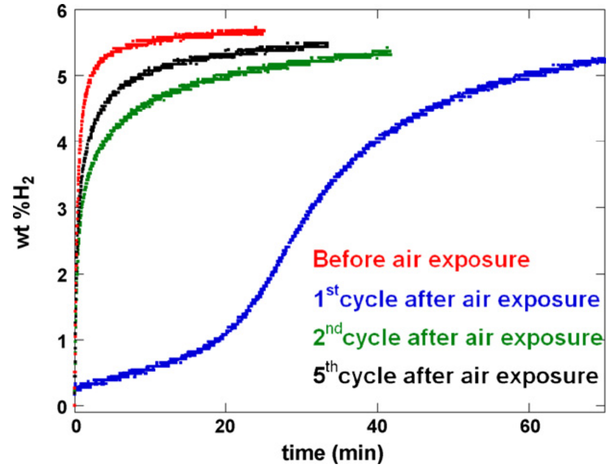

Fig. 8. Absorption traces successively recorded on a damaged specimen (MgH_2 + 5 at.% V). The outgassed powder has been exposed to air atmosphere at 300 °C for 10 min.

In a second step, thermal annealing of 100 h have been performed on desorbed powders at temperatures ranging from 300 to 400 °C. As observed on Fig. 9, sorption kinetics remain unchanged up to 350 °C, whereas a strong change in the sorption behaviour is observed after annealing between 370 and 380 °C, with a sharp decrease of kinetics, due to the rapid crystal growth of Mg crystallites above this temperature. Then, it appears very important not to exceed this critical temperature of 370 °C within the tank.

5. Pilot tank development

The hydriding/dehydriding of Mg are strongly exothermic/endothermic reactions. Then, the main difficulty to solve for

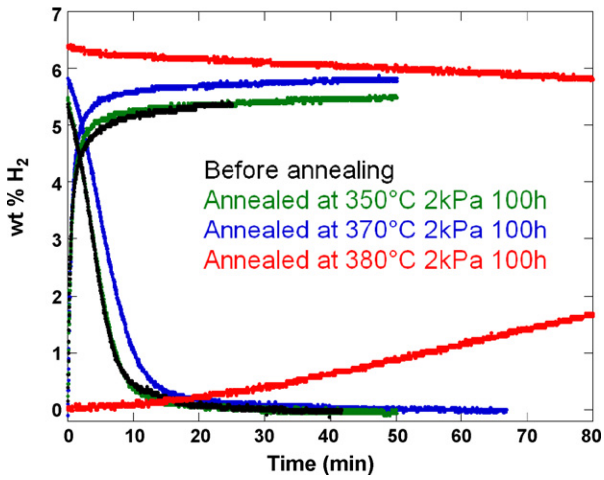

Fig. 9. Kinetic traces for powders ball milled for 8 h at MCP T and aged for 100 h at 350, 370 and 380 °C, respectively.

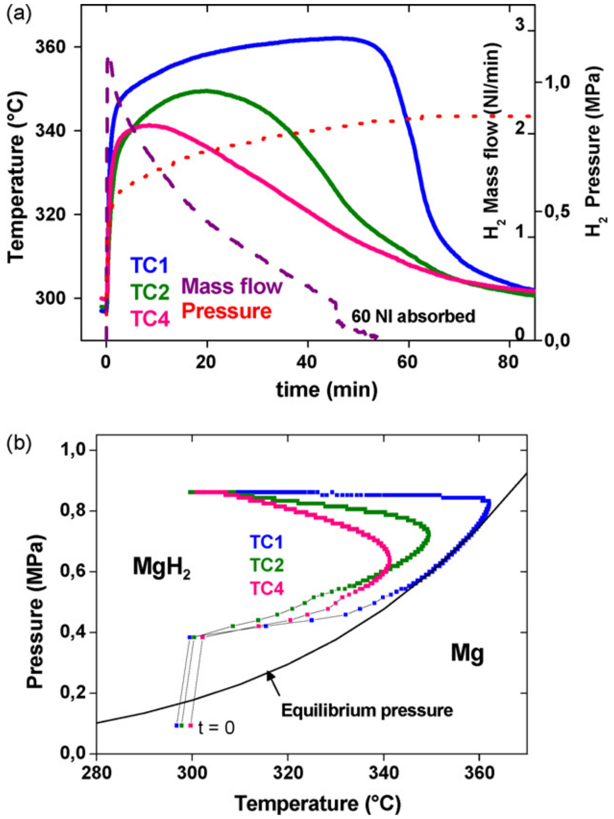

Fig. 10. (a) Hydrogen pressure and temperatures evolution loading the MgH_2 tank, and (b) recorded hydrogen pressure vs. temperatures as compared to the PCT diagram.

the development of MgH_2 based tank is to control the heat flow (extraction of the heat during charging, and maintaining the tank above the equilibrium temperature when discharging). A small-scale tank ($V = 260\,cm^3$) filled with 110 gr of activated MgH_2 powder has been developed. This tank is cylindrical to minimize uncontrolled heat exchange and to ease numerical modeling. It is heated from outside (up to 400 °C). Inside pressure, H_2 mass flow and temperatures measured in different part of the tank are recorded. The behaviour has been studied upon various experimental conditions (temperature, H_2 pressure, cooling fluid, cycling, etc.).

5.1. Charging process

The first absorption tests were performed at 280 °C without cooling fluid in the exchangers. The introduction of hydrogen produces a sharp increase of temperature as measured in all the different parts of the tank (Fig. 10a), so that the temperature immediately reaches the equilibrium conditions (Fig. 10b). After a few minutes, the thermocouples TC 3 and 4 (external part, top and bottom) take off the equilibrium trace: hydrogen absorption has excellent kinetics in the external region of the tank. On the contrary, in the central part of the tank (TC 1), almost 1 h is needed to auto-cool down the powder since the local temperature follows the equilibrium curve until the end of absorption. When starting absorption at 280 °C, 60 Nl H_2 have been absorbed, corresponding to a capacity of 4.9 wt.% H_2.

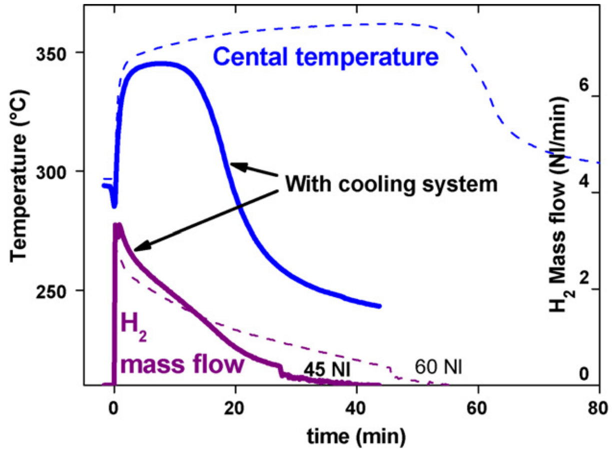

Fig. 11. Comparison of the central temperatures (blue) and hydrogen mass flow (purple) evolution loading the MgH_2 tank, with (straight lines) and without cooling system (dashed lines).

Further experiments have been performed using water or compressed air as cooling fluids. By removing the heat generated by the hydriding reaction, the cooling system reduces the tank-loading time. In Fig. 11, the mass flow and the central temperature recorded with and without compressed air are reported. Less than 30 min are now needed to load the tank, but only 45 Nl H_2 are absorbed (3.65 wt.%. H_2), the cooling being too efficient at the end of the reaction. Compressed air seems to be a quite good solution as it offers a good efficiency with a reduced mass flow (∼10 Nl/min). However, mass flow management is needed to carry the reaction on to the end.

5.2. Discharging process

Desorption experiments have been carried out between 350 and 400 °C where the outlet pressure is the atmospheric pressure. As observed on Fig. 12, an important decrease of temperature appears in the center part of the tank (endothermic reaction). Due to this decrease of temperature, and to maintain a reasonable mass flow, a desorption temperature of 350 °C is needed for the present geometrical configuration. However, heating directly the center part of the tank could allow reducing the temperature.

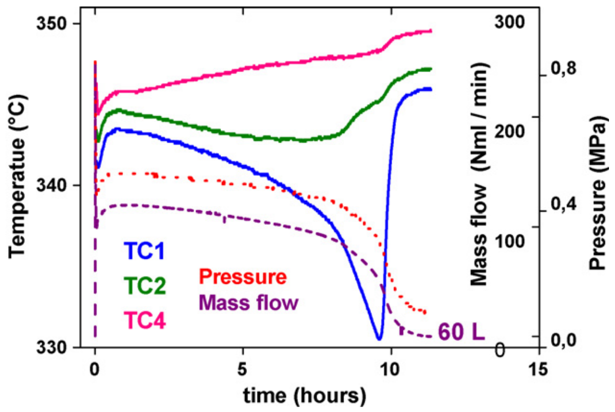

Fig. 12. Hydrogen pressure, mass flow and temperatures evolution during discharging of the MgH_2 tank.

For both absorption and desorption steps, the very low thermal conductivity of the powder and the thermal expansion slow down the reaction by preventing heat transfer. The use of expanded natural graphite or metallic foam matrix is expected to increase the reaction rate due to improve thermal conduction.

6. Conclusion

A systematic investigation on MgH_2 co-milled with transition metals M for increasing milling time has identified the successive MH_x hydrides formed by reaction with MgH_2. The initiating role of the metal hydride MH_x has been evidenced by neutron diffraction experiments. The co-milling conditions were transferred to MCP Technologies SA, where highly reactive batches of powders were processed. Moreover, a specimen accidentally exposed to air was shown to recover the initial properties after a few cycles performed under hydrogen. However, it has been demonstrated that it is essential to maintain the material below 370 °C to avoid the rapid crystal growth of the Mg particles associated to a strong degradation of the kinetics of the hydriding/dehydriding reactions.

A small-scale tank was developed and tested in different cooling conditions. Starting at 280 °C, 60 Nl H_2 have been absorbed, corresponding to a capacity of 4.9 wt.%. Numerical simulations mapping the heat and mass transfers during the hydrogenation/dehydrogenation steps are in progress using the Fluent software. A systematic comparison with experimental data will allow a better understanding of the tank behaviour.

Acknowledgements

Partial funding by the European Commission DG Research (contracts ENK6-CT-2002-00600 HYSTORY and SES6-2006-518271/NESSHY) is gratefully acknowledged by the authors.

References

[1] J. Huot, G. Liang, S. Boily, A. van Neste, R. Schultz, J. Alloys Compd. 293–295 (1999) 495.

[2] L. Zaluski, A. Zaluska, J.O. Strom-Olsen, J. Alloys Compd. 253–254 (1997) 70.

[3] G. Liang, J. Huot, S. Boily, A. van Neste, R. Schultz, J. Alloys Compd. 292 (1999) 247.

[4] W. Oelerich, T. Klassen, R. Bormann, J. Alloys Compd. 315 (2001) 237.

[5] A. Jemni, S. Ben Nasrallah, Int. J. Hydrogen Energy 20 (1) (1995) 43–52.

[6] M. Pons, P. Dantzer, Int. J. Hydrogen Energy 19 (7) (1994) 611–616.

[7] A. Jemni, S. Ben Nasrallah, J. Lamloumi, Int. J. Hydrogen Energy 24 (1999) 631–644.

[8] A. Demircan, M. Demiralp, Y. Kaplan, M.D. Mat, T.N. Veziroglu, Int. J. Hydrogen Energy 30 (2005) 1437–1446.

[9] J.F. Pelletier, J. Huot, M. Sutton, R. Schulz, A.R. Sandy, L.B. Lurio, S.G.M. Mochrie, Phys. Rev. B 63 (2001) 052103.

[10] O. Friedrichs, J.C. Sanchez-Lopez, C. Lopez-Cartes, M. Dornhiem, T. Klassen, R. Bormann, A. Fernandez, Appl. Surf. Sci. 252 (2006) 2334–2345.